Measurement of the prompt-production cross-section ratio σ (χ c 2) / σ (χ c 1) in p Pb collisions at √ s N N = 8.16 TeV

De Bruyn, K.; Onderwater, C. J. G.; van Veghel, M.; LHCb Collaboration

Published in:
Physical Review C

DOI:
10.1103/PhysRevC.103.064905

Publication date:
2021

Citation for published version (APA):
De Bruyn, K., Onderwater, C. J. G., van Veghel, M., & LHCb Collaboration (2021). Measurement of the prompt-production cross-section ratio σ (χ c 2) / σ (χ c 1) in p Pb collisions at √ s N N = 8.16 TeV. *Physical Review C*, *103*(6), [064905]. https://doi.org/10.1103/PhysRevC.103.064905

PHYSICAL REVIEW C **103**, 064905 (2021)

Measurement of the prompt-production cross-section ratio $\sigma(\chi_{c2})/\sigma(\chi_{c1})$ in pPb collisions at $\sqrt{s_{NN}} = 8.16$ TeV

R. Aaij *et al.**
(LHCb Collaboration)

(Received 17 March 2021; accepted 23 April 2021; published 9 June 2021)

This article reports the first measurement of prompt χ_{c1} and χ_{c2} charmonium production in nuclear collisions at Large Hadron Collider energies. The cross-section ratio $\sigma(\chi_{c2})/\sigma(\chi_{c1})$ is measured in pPb collisions at $\sqrt{s_{NN}} = 8.16$ TeV, collected with the LHCb experiment. The $\chi_{c1,2}$ states are reconstructed via their decay to a J/ψ meson, subsequently decaying into a pair of oppositely charged muons, and a photon, which is reconstructed in the calorimeter or via its conversion in the detector material. The cross-section ratio is consistent with unity in the two considered rapidity regions. Comparison with a corresponding cross-section ratio previously measured by the LHCb Collaboration in pp collisions suggests that χ_{c1} and χ_{c2} states are similarly affected by nuclear effects occurring in pPb collisions.

DOI: 10.1103/PhysRevC.103.064905

I. INTRODUCTION

Collisions of protons with nuclei offer opportunities to study the production and interaction of heavy quarks inside the nucleus. Charm-quark production in hadron collisions is sensitive to the gluon content of colliding hadrons, and can be used to probe modifications of the parton distributions inside the nucleus [1]. While traversing the nucleus, heavy quarks are also subject to energy loss that can lead to the suppression of bound states [2]. Once the heavy-quark pair exits the nucleus, late-stage interactions with comoving hadrons can disrupt fully formed quarkonium states [3]. Measurements in proton-nucleus collisions also give an experimental baseline for the interpretation of quarkonium suppression in nucleus-nucleus collisions, where color screening in a deconfined quark-gluon plasma is expected to be a dominant effect [4]. Studies of quarkonium suppression in pPb collisions revealed that the excited states, such as the charmonium $\psi(2S)$ state or the bottomonium $\Upsilon(2S)$ and $\Upsilon(3S)$ states, show a different suppression pattern compared to the J/ψ and $\Upsilon(1S)$ states (see [5–11] and references therein). Such a difference cannot be explained by processes taking place during the initial stages of the collision, i.e., acting on the quark-antiquark pair. Instead, the processes must occur after the hadronization of the heavy-quark pair into a final state, e.g., through dissociation due to interactions with the comoving matter created at the collision point [12,13]. Currently, the J/ψ and $\psi(2S)$ mesons are the only charmonium states which have been measured in collisions of protons with nuclei at the Large Hadron Collider (LHC).

The χ_{cJ} states, with $J = 0, 1, 2$ denoting the total angular momentum, comprise a triplet of orbitally excited $1P$ charmonia. They are typically studied in collider experiments via their radiative decay $\chi_{cJ} \to J/\psi\gamma$, with a subsequent decay $J/\psi \to \ell^+\ell^-$, where ℓ denotes electron or muon. A selection of recent measurements in pp and $p\overline{p}$ collisions can be found in Refs. [14–18].

The binding energies of χ_{cJ} states are significantly smaller than that of the J/ψ state and greater than the binding energy of $\psi(2S)$ state [19]. The small difference in the binding energies of χ_{c1} and χ_{c2} charmonia makes the ratio of their production cross sections, $\sigma(\chi_{c2})/\sigma(\chi_{c1})$, a useful tool to study their sensitivity to final-state nuclear effects, which are expected to be similar for both states. The χ_{cJ} states also form an important feed-down contribution to J/ψ production, so measurements of nuclear effects on χ_{cJ} states can clarify interpretation of the J/ψ data. Moreover, various efficiency factors and sources of uncertainty cancel out in the ratio, allowing for a more precise measurement. In nuclear collisions, the χ_{cJ} states have been measured by the HERA-B [20] and PHENIX Collaborations [21]. To date, no measurement has been reported at the LHC energies.

Here we present the first measurement of the cross-section ratio of promptly produced χ_{c2} and χ_{c1} states, $\sigma(\chi_{c2})/\sigma(\chi_{c1})$, in nuclear collisions at the LHC. The measurement is performed using data collected by the LHCb Collaboration in pPb collisions, at the center-of-mass energy per nucleon pair $\sqrt{s_{NN}} = 8.16$ TeV, in 2016.

II. EXPERIMENTAL APPARATUS

The LHCb detector [22,23] is a single-arm forward spectrometer covering the pseudorapidity range $2 < \eta < 5$, designed for the study of particles containing b or c quarks. The detector consists of a high-precision silicon-strip vertex

---

*Full author list given at the end of the article.

locator (VELO) surrounding the interaction region, a set of four planar tracking stations coupled to a dipole magnet with a 4 Tm bending power, a pair of ring-imaging Cherenkov detectors to discriminate between different types of charged hadrons, followed by calorimetric and muon systems that are of particular importance in this measurement. The calorimetric system allows for identification of electrons and photons and consists of a scintillating pad detector (SPD), a preshower system (PS), an electromagnetic (ECAL) calorimeter, and a hadronic (HCAL) calorimeter. The SPD and PS are designed to discriminate between signals from photons and electrons, while ECAL and HCAL provide the energy measurement and identify electromagnetic radiation and neutral hadrons. Muons are identified by a system composed of alternating layers of iron and multiwire proportional chambers.

The pPb data were collected with the LHCb experiment in two distinct beam configurations. In the forward configuration, the particles produced in the direction of the proton beam are measured in a center-of-mass rapidity region $1.5 < y^* < 4.0$, while, in the backward configuration, particles produced in the lead-beam direction are measured at center-of-mass rapidity $-5.0 < y^* < -2.5$. The forward (backward) data sample corresponds to an integrated luminosity of about 14 $\mu\mathrm{b}^{-1}$ (21 $\mu\mathrm{b}^{-1}$).

III. DATA SELECTION

The analyzed events are selected by a set of triggers designed to record collisions containing the decay $J/\psi \to \mu^+\mu^-$. The J/ψ candidates are reconstructed from a pair of oppositely charged muons with momentum component transverse to the beam, p_T, larger than 700 MeV/c, originating from a common vertex and an invariant mass within ± 42 MeV/c^2 of the known J/ψ mass [24] (corresponding to three times the dimuon mass resolution). The J/ψ candidates are combined with a photon candidate to form a $\chi_{c1,2}$ candidate. Photons used in this analysis are classified in two mutually exclusive types: those that converted in the detector material upstream of the dipole magnet and of which the electron and positron tracks were reconstructed in the tracking system (*converted photons*), or those reconstructed through their energy deposits in the calorimetric system (*calorimetric photons*). The calorimetric photon sample is about an order of magnitude larger than the converted photon sample but has worse mass resolution. Converted photons are reconstructed from a pair of oppositely charged electron candidates and are required to have a transverse momentum $p_\mathrm{T} > 600$ MeV/c and a good-quality conversion vertex $\gamma \to e^+e^-$. Calorimetric photons are identified using the ratio of their energy deposited in the hadronic and electromagnetic calorimeters and a pair of likelihood-based classifiers that discriminate photons from electrons and hadrons [25,26]. Calorimetric photons accepted for analysis are required to have $p_\mathrm{T} > 1$ GeV/c. The two measurements discussed here are independent given the different reconstruction between the converted and the calorimetric photons. The selected $\mu^+\mu^-\gamma$ combinations, which comprise the $\chi_{c1,2}$ candidates, are required to be reconstructed within the pseudorapidity window $2 < \eta < 4.5$ and in the transverse momentum range of $3 < p_\mathrm{T} < 15$ GeV/c for the converted and $5 < p_\mathrm{T} < 15$ GeV/c for the calorimetric candidates. In order to select the $\chi_{c1,2}$ candidates produced *promptly* at the primary-collision vertex and to suppress *nonprompt* production from b-hadron decays occurring away from the primary vertex, an upper limit is imposed on the pseudodecay time of the candidates, defined as

$$t_z = \frac{(z_\mathrm{decay} - z_\mathrm{PV}) \times M_{\chi_{c1}}}{p_z}, \tag{1}$$

where $z_\mathrm{decay} - z_\mathrm{PV}$ is the difference between the positions of the reconstructed vertex of the $\chi_{c1,2}$ candidate and the primary proton-nucleus collision vertex along the beam axis, p_z is the longitudinal component of the $\chi_{c1,2}$ candidate momentum and $M_{\chi_{c1}}$ is the known mass of the χ_{c1} meson [24]. The pseudodecay time is limited to $t_z < 0.1$ ps. The χ_{c1} and χ_{c2} candidates originating from decays of short-lived resonances, such as $\psi(2S)$ produced at the interaction point, are also considered in the analysis.

The effects of the detector acceptance as well as of the reconstruction and selection efficiencies are investigated with simulated events. The $\chi_{c1,2}$ signal is generated in PYTHIA [27] with an LHCb specific configuration [28]. The χ_{c1} and χ_{c2} states are generated assuming unpolarized production. The underlying minimum bias forward and backward pPb collisions are generated using the EPOS event generator configured for the LHC [29]. Unstable particles are decayed via EVTGEN [30]. The $J/\psi \to \mu^+\mu^-$ decays are corrected for final-state electromagnetic radiation using PHOTOS [31]. The response of the detector to the interactions of the generated particles is implemented using the GEANT4 toolkit [32]; for a detailed description see Ref. [33].

IV. DATA ANALYSIS

This paper aims at measuring the ratio of the cross sections for prompt χ_{c1} and χ_{c2} production. The cross-section ratio is defined as

$$\frac{\sigma(\chi_{c2})}{\sigma(\chi_{c1})} = \frac{N_{\chi_{c2}}}{N_{\chi_{c1}}} \frac{\varepsilon_{\chi_{c1}}}{\varepsilon_{\chi_{c2}}} \frac{\mathcal{B}(\chi_{c1} \to J/\psi\gamma)}{\mathcal{B}(\chi_{c2} \to J/\psi\gamma)}. \tag{2}$$

Here, $N_{\chi_{c2}}$ and $N_{\chi_{c1}}$ represent the signal yields of the χ_{c2} and χ_{c1} states, respectively, and $\varepsilon_{\chi_{c2}}$ and $\varepsilon_{\chi_{c1}}$ denote the efficiencies to reconstruct and select the corresponding state. The branching fractions for the $\chi_{c1,2}$ decays are $\mathcal{B}(\chi_{c1} \to J/\psi\gamma) = (34.3 \pm 1.0)\%$ and $\mathcal{B}(\chi_{c2} \to J/\psi\gamma) = (19.0 \pm 0.5)\%$ [24].

The χ_{c1} and χ_{c2} signal yields are determined by performing a binned maximum-likelihood fit to the spectra of the difference between the invariant mass of the $\mu^+\mu^-\gamma$ candidate and that of the $\mu^+\mu^-$ pair, $\Delta M \equiv M(\mu^+\mu^-\gamma) - M(\mu^+\mu^-)$. The fit function comprises a Gaussian shape for the χ_{c1} and χ_{c2} resonances and a background component described with a second-order Chebyshev polynomial. In the fit, the difference between the values of the χ_{c1} and χ_{c2} masses is set to the known mass difference [24]. The widths of the χ_{c1} and χ_{c2} peaks are set to be equal, following expectations from simulation, and left as a free parameter. The χ_{c0} peak is also included in the fit, however no significant χ_{c0} yield is observed. The fit to the spectra of converted candidates is performed in the range $200 < \Delta M < 800$ (850) MeV/c^2 at forward (backward) rapidity. For the calorimetric candidates, the invariant-mass difference spectrum is fitted

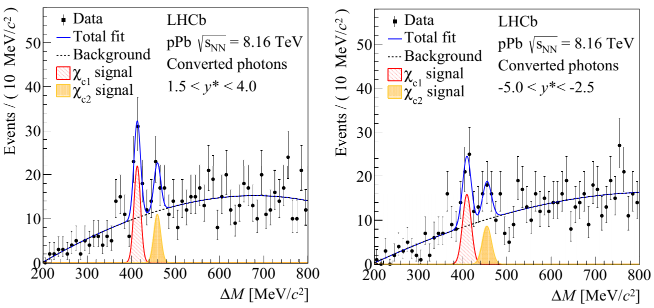

FIG. 1. Mass-difference spectra of converted $\chi_{c1,2}$ candidates in forward (left) and backward (right) configuration data. The data are superimposed with a fit (solid blue line) comprising χ_{c1} and χ_{c2} signals and combinatorial background (dashed black line).

between $250 < \Delta M < 650$ MeV$/c^2$ in the two rapidity intervals. The mass-difference spectra of the converted and calorimetric samples are shown, together with the fit components, in Figs. 1 and 2, respectively. In the converted samples, the yield ratio $N_{\chi_{c2}}/N_{\chi_{c1}}$ is determined to be 0.51 ± 0.23 at forward and 0.56 ± 0.26 at backward rapidity, where the uncertainties are statistical. In the calorimetric samples, these ratios are found to be 0.63 ± 0.08 at forward and 0.67 ± 0.10 at backward rapidity. Individual yields as well as their corresponding significance are listed in Table I.

Since the kinematics of χ_{c1} and χ_{c2} decays are nearly identical, various detector effects such as tracking and particle-identification efficiencies cancel out in the ratio, so that the efficiency ratio in Eq. (2) can be expressed as

$$\frac{\varepsilon_{\chi_{c1}}}{\varepsilon_{\chi_{c2}}} = \frac{\varepsilon^{\mathrm{acc}}_{\chi_{c1}}}{\varepsilon^{\mathrm{acc}}_{\chi_{c2}}}\frac{\varepsilon^{\mathrm{reco}}_{\chi_{c1}}}{\varepsilon^{\mathrm{reco}}_{\chi_{c2}}}.$$

The factor $\varepsilon^{\mathrm{acc}}$ expresses the geometrical acceptance of the decay products to fall within the LHCb acceptance, while the factor $\varepsilon^{\mathrm{reco}}$ represents the efficiency of selection and reconstruction of the signal candidates. These correction factors are computed from dedicated simulated events.

V. SYSTEMATIC UNCERTAINTIES

The systematic uncertainties on the cross-section ratios are determined as follows. A systematic uncertainty on the signal extraction is determined by varying the models used in the mass-difference fits. Several different signal and background models are tested. The signal shapes are varied between Gaussian functions and Voigtian functions (a convolution of a Breit-Wigner and a Gaussian function), and the background shape is varied between second- and third-order Chebyshev polynomials. The natural widths of the χ_{c1} and χ_{c2} states are narrow compared to the resolution; the Breit-Wigner widths are therefore fixed to the known values [24]. The fit range is varied between $100\ (150) < \Delta M < 900$ MeV/c^2 and $200 < \Delta M < 800\ (850)$ MeV/c^2 for the converted candidates at forward (backward) rapidity. For the calorimetric candidates, the fit range is varied between $250 < \Delta M < 650$ MeV/c^2 and $300 < \Delta M < 600$ MeV/c^2 in the two rapidity intervals. The various choices of signal shape, background parametrization, and range give a total of eight fits to each of the mass-difference spectra in each rapidity interval. In all cases, the χ_{c0} peak is also included in the fit; however, no significant χ_{c0} yield is observed. The systematic uncertainty on the yield ratios due to the fitting procedure is assigned as the standard deviation between the values returned by the eight individual fits. For the converted sample, this systematic uncertainty amounts to 4.9% (3.2%) at forward (backward) rapidity. For the calorimetric sample it is 2.6% (6.8%) at forward (backward) rapidity. The residual background from the nonprompt $\chi_{c1,2}$ production is verified as negligible and shown to cancel out in the ratio, hence no related uncertainty is assigned. The systematic uncertainty on the acceptance and efficiency corrections includes contributions from the limited size of the simulated samples used to compute the $\varepsilon^{\mathrm{acc}}$ and $\varepsilon^{\mathrm{reco}}$ factors, and the uncertainty due to the discrepancy of the $\chi_{c1,2}$ and photon properties between data and simulation. The latter is estimated using simulated samples, weighted to reproduce the kinematic distributions of $\chi_{c1,2}$ and photons in background-subtracted data, and obtained using the *sPlot* technique, with ΔM as the discriminating variable [34]. The weights are extracted by comparing the transverse momentum and rapidity dependent ratios of the simulated counts $N_{\chi_{c1}}/N_{\chi_{c2}}$ with those in data. The simulated χ_{c1} samples are then weighted event-by-event and the uncertainty is assessed as the difference between the efficiency ratios computed from simulated samples prior to and after weighting. In the case of calorimetric photons, an additional weighting process is required in order to recover kinematic distributions of final-state photons observed in the data as well, in a similar event-by-event process as the weights obtained from $\chi_{c1,2}$ kinematic distributions. The effect of the photon-identification selection and the reproducibility of relevant variables in simulation are also taken into account. For the converted $\chi_{c1,2}$ sample, the total systematic uncertainty on the acceptance and efficiency equals 9.6% at forward and 14.9% at backward rapidity, while for the calorimetric sample the uncertainty is 8.1% at forward rapidity and 12.4% at backward rapidity. The ratio of the branching fractions of the $\chi_{c1,2} \to J/\psi\gamma$ decays contributes with an uncertainty of 3.9%. A summary of contributions to the statistical and systematic uncertainties of each analyzed sample is given in Table II.

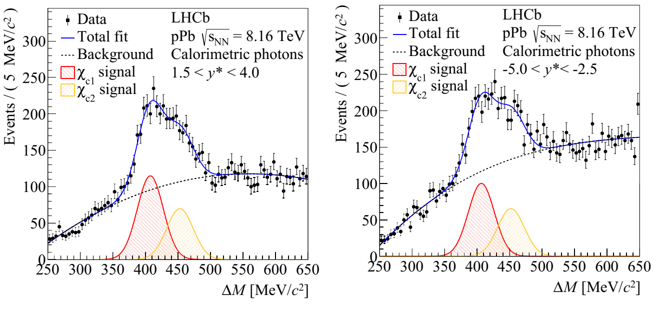

FIG. 2. Mass-difference spectra of calorimetric $\chi_{c1,2}$ candidates in forward (left) and backward (right) data. The data are superimposed with a fit result (solid blue line) comprising χ_{c1} and χ_{c2} signals and combinatorial background (dashed black line).

TABLE I. Yields of χ_{c1} and χ_{c2} signals with statistical uncertainties and corresponding significance (given in standard deviations).

Data sample		$N_{\chi_{c1}}$	Significance	$N_{\chi_{c2}}$	Significance
Converted photons	$1.5 < y^* < 4.0$	41 ± 9	6.0	21 ± 8	3.1
	$-5.0 < y^* < -2.5$	38 ± 9	4.4	21 ± 8	3.0
Calorimetric photons	$1.5 < y^* < 4.0$	1151 ± 69	15.7	721 ± 76	9.8
	$-5.0 < y^* < -2.5$	1004 ± 73	13.3	676 ± 82	8.5

VI. RESULTS

The prompt-production cross-section ratio $\sigma(\chi_{c2})/\sigma(\chi_{c1})$ in *p*Pb collisions at the center-of-mass energy per nucleon pair $\sqrt{s_{NN}} = 8.16$ TeV is shown for the two rapidity regions in Fig. 3. The ratio measured from converted photons amounts to

$$\frac{\sigma(\chi_{c2})}{\sigma(\chi_{c1})} = 0.92 \pm 0.42\ (\text{stat.}) \pm 0.11\ (\text{syst.}) \quad \text{for } 1.5 < y^* < 4.0,$$

$$\frac{\sigma(\chi_{c2})}{\sigma(\chi_{c1})} = 0.98 \pm 0.46\ (\text{stat.}) \pm 0.15\ (\text{syst.}) \quad \text{for } -5.0 < y^* < -2.5.$$

The ratio measured from calorimetric photons is found to be

$$\frac{\sigma(\chi_{c2})}{\sigma(\chi_{c1})} = 1.11 \pm 0.14\ (\text{stat.}) \pm 0.10\ (\text{syst.}) \quad \text{for } 1.5 < y^* < 4.0,$$

$$\frac{\sigma(\chi_{c2})}{\sigma(\chi_{c1})} = 1.14 \pm 0.16\ (\text{stat.}) \pm 0.17\ (\text{syst.}) \quad \text{for } -5.0 < y^* < -2.5.$$

The cross-section ratios for both converted and calorimetric samples are consistent with unity in both rapidity regions. The significantly larger yield of the calorimetric sample allows more precise conclusions on the observed trend to be drawn.

The cross-section ratio obtained in *p*Pb data is compared with the corresponding ratio measured in *pp* collisions at $\sqrt{s} = 7$ TeV by the LHCb Collaboration [16]. The two measurements are consistent within two standard deviations. While the ratio in the *pp* data was measured at a lower center-of-mass energy than that of *p*Pb collisions, results show that the relative cross section of different charmonium states is independent of energy at the LHC energy scale [35]. Thus, the only aspect to consider in a direct comparison between the shown *p*Pb and *pp* data is the rapidity range, where the *p*Pb results are shifted by -0.5 in rapidity. Bearing that in mind, we can express the relative suppression of χ_{c2} and χ_{c1} states via the ratio of their nuclear-modification factors,

$$\mathcal{R} \equiv \frac{\sigma(\chi_{c2})/\sigma(\chi_{c1})|_{p\text{Pb}}}{\sigma(\chi_{c2})/\sigma(\chi_{c1})|_{pp}}. \tag{3}$$

Using the more precise calorimetric *p*Pb results, the ratio of nuclear-modification factors amounts to $\mathcal{R} = 1.41 \pm 0.21(\text{stat.}) \pm 0.18(\text{syst.})$ at forward and $\mathcal{R} = 1.44 \pm 0.24(\text{stat.}) \pm 0.25(\text{syst.})$ at backward rapidity, showing no significant change relative to the *pp* ratio in either rapidity region. The measured cross-section ratio and ratio of nuclear-modification factors suggest that the nuclear effects have the same impact on both χ_{c1} and χ_{c2} states within uncertainties, independent of rapidity.

TABLE II. Statistical and systematic uncertainties on the cross-section ratio, $\sigma(\chi_{c2})/\sigma(\chi_{c1})$. The total systematic uncertainty is also quoted.

Analyzed sample	Source	$1.5 < y^* < 4.0$	$-5.0 < y^* < -2.5$
Converted photons	Signal extraction	4.9%	3.2%
	Limited simulation sample size	5.6%	6.5%
	Efficiency correction	7.7%	13.4%
	Branching fraction ratio	3.9%	3.9%
	Total systematic uncertainty	11.4%	15.7%
	Statistical uncertainty	45.2%	47.0%
Calorimetric photons	Signal extraction	2.6 %	6.8%
	Limited simulation sample size	2.5%	2.8%
	Efficiency correction	7.7%	12.1%
	Branching fraction ratio	3.9%	3.9%
	Total systematic uncertainty	9.3%	14.7%
	Statistical uncertainty	12.2%	14.2%

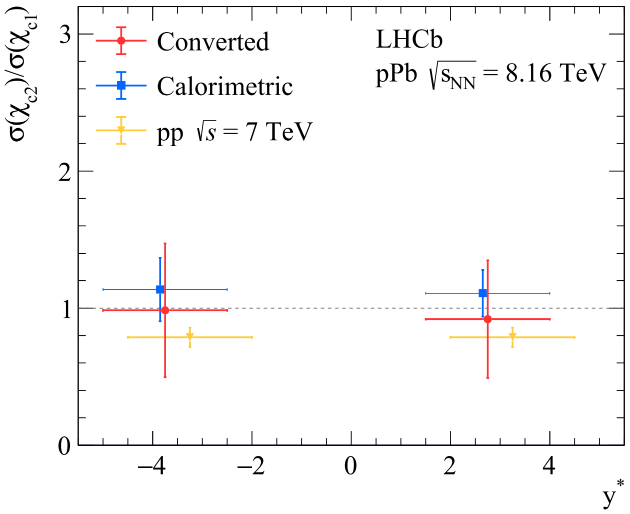

FIG. 3. Cross-section ratio, $\sigma(\chi_{c2})/\sigma(\chi_{c1})$ as a function of center-of-mass rapidity y^*, for the χ_{c2} and χ_{c1} promptly produced in pPb collisions measured using converted photons (red circles) and calorimetric photons (blue squares). The error bars correspond to the total uncertainties. Blue points and vertical uncertainties are shifted horizontally to improve visibility. The pPb data are compared with results of the converted sample in pp collisions at $\sqrt{s} = 7$ TeV [16] (yellow triangles).

VII. SUMMARY

In summary, we present the first measurement of $\chi_{c1,2}$ charmonium production in nuclear collisions at the LHC. The cross-section ratio $\sigma(\chi_{c2})/\sigma(\chi_{c1})$ is consistent with unity for both forward and backward rapidity regions. Moreover, comparison with the ratio measured in pp collisions hints at a suppression pattern between the two states, which is comparable within uncertainties. This suggests that the final-state nuclear effects impact the χ_{c1} and χ_{c2} states similarly within the achieved precision.

ACKNOWLEDGMENTS

We express our gratitude to our colleagues in the CERN accelerator departments for the excellent performance of the LHC. We thank the technical and administrative staff at the LHCb institutes. We acknowledge support from CERN and from the national agencies: CAPES, CNPq, FAPERJ, and FINEP (Brazil); MOST and NSFC (China); CNRS/IN2P3 (France); BMBF, DFG, and MPG (Germany); INFN (Italy); NWO (Netherlands); MNiSW and NCN (Poland); MEN/IFA (Romania); MSHE (Russia); MICINN (Spain); SNSF and SER (Switzerland); NASU (Ukraine); STFC (United Kingdom); DOE NP and NSF (USA). We acknowledge the computing resources that are provided by CERN, IN2P3 (France), KIT and DESY (Germany), INFN (Italy), SURF (Netherlands), PIC (Spain), GridPP (United Kingdom), RRCKI and Yandex LLC (Russia), CSCS (Switzerland), IFIN-HH (Romania), CBPF (Brazil), PL-GRID (Poland), and NERSC (USA). We are indebted to the communities behind the multiple open-source software packages on which we depend. Individual groups or members have received support from ARC and ARDC (Australia); AvH Foundation (Germany); EPLANET, Marie Skłodowska-Curie Actions, and ERC (European Union); A*MIDEX, ANR, Labex P2IO and OCEVU, and Région Auvergne-Rhône-Alpes (France); Key Research Program of Frontier Sciences of CAS, CAS PIFI, CAS CCEPP, Fundamental Research Funds for the Central Universities, and Sci. & Tech. Program of Guangzhou (China); RFBR, RSF, and Yandex LLC (Russia); GVA, XuntaGal, and GENCAT (Spain); the Leverhulme Trust, the Royal Society, and UKRI (United Kingdom).

[1] R. Vogt, Shadowing and absorption effects on J/ψ production in dA collisions, Phys. Rev. C **71**, 054902 (2005).

[2] F. Arleo and S. Peigné, Heavy-quarkonium suppression in p-A collisions from parton energy loss in cold QCD matter, J. High Energy Phys. 03 (2013) 122.

[3] A. Capella, A. Kaidalov, A. K. Akil, and C. Gerschel, J/ψ and ψ' suppression in heavy ion collisions, Phys. Lett. B **393**, 431 (1997).

[4] T. Matsui and H. Satz, J/ψ suppression by quark-gluon plasma formation, Phys. Lett. B **178**, 416 (1986).

[5] R. Aaij *et al.* (LHCb Collaboration), Prompt and nonprompt J/ψ production and nuclear modification in pPb collisions at $\sqrt{s_{NN}} = 8.16$ TeV, Phys. Lett. B **774**, 159 (2017).

[6] R. Aaij *et al.* (LHCb Collaboration), Study of $\psi(2S)$ production cross-sections and cold nuclear matter effects in pPb collisions at $\sqrt{s_{NN}} = 5$ TeV, J. High Energy Phys. 03 (2016) 133.

[7] A. Adare *et al.* (PHENIX Collaboration), Measurement of the relative yields of $\psi(2S)$ to $\psi(1S)$ mesons produced at forward and backward rapidity in p+p, p+Al, p+Au, and ^{3}He+Au collisions at $\sqrt{s_{NN}} = 200$ GeV, Phys. Rev. C **95**, 034904 (2017).

[8] R. Aaij *et al.* (LHCb Collaboration), Study of Υ production in pPb collisions at $\sqrt{s_{NN}} = 8.16$ TeV, J. High Energy Phys. 11 (2018) 194.

[9] S. Acharya *et al.* (ALICE Collaboration), Measurement of nuclear effects on $\psi(2S)$ production in p-Pb collisions at $\sqrt{s_{\rm NN}} = 8.16$ TeV, J. High Energy Phys. 07 (2020) 237.

[10] M. Aaboud *et al.* (ATLAS Collaboration), Measurement of quarkonium production in proton–lead and proton–proton collisions at 5.02 TeV with the ATLAS detector, Eur. Phys. J. C **78**, 171 (2018).

[11] A. M. Sirunyan *et al.* (CMS Collaboration), Measurement of prompt $\psi(2S)$ production cross sections in protonlead and protonproton collisions at $\sqrt{s_{\rm NN}} = 5.02$ TeV, Phys. Lett. B **790**, 509 (2019).

[12] E. G. Ferreiro, Excited charmonium suppression in proton–nucleus collisions as a consequence of comovers, Phys. Lett. B **749**, 98 (2015).

[13] E. G. Ferreiro and J.-P. Lansberg, Is bottomonium suppression in proton-nucleus and nucleus-nucleus collisions at LHC energies due to the same effects? J. High Energy Phys. 10 (2018) 094; 03 (2019) 063(E).

[14] A. Abulencia *et al.* (CDF Collaboration), Measurement of $\sigma_{\chi_{c2}}\mathcal{B}(\chi_{c2} \to J/\psi\gamma)/\sigma_{\chi_{c1}}\mathcal{B}(\chi_{c1} \to J/\psi\gamma)$ in $p\bar{p}$ Collisions at $\sqrt{s} = 1.96$ TeV, Phys. Rev. Lett. **98**, 232001 (2007).

[15] R. Aaij *et al.* (LHCb Collaboration), Measurement of the cross-section ratio $\sigma(\chi_{c2})/\sigma(\chi_{c1})$ for prompt χ_c production at $\sqrt{s}$ =7 TeV, Phys. Lett. B **714**, 215 (2012).

[16] R. Aaij *et al.* (LHCb Collaboration), Measurement of the relative rate of prompt χ_{c0}, χ_{c1} and χ_{c2} production at $\sqrt{s} = 7$ TeV, J. High Energy Phys. 10 (2013) 115.

[17] S. Chatrchyan *et al.* (CMS Collaboration), Measurement of the relative prompt production rate of χ_{c2} and χ_{c1} in *pp* collisions at $\sqrt{s} = 7$ TeV, Eur. Phys. J. C **72**, 2251 (2012).

[18] A. Adare *et al.* (PHENIX Collaboration), Ground and excited charmonium state production in $p + p$ collisions at $\sqrt{s} =$ 200 GeV, Phys. Rev. D **85**, 092004 (2012).

[19] H. Satz, Colour deconfinement and quarkonium binding, J. Phys. G **32**, R25 (2006).

[20] I. Abt *et al.* (HERA-B Collaboration), Production of the charmonium states χ_{c1} and χ_{c2} in proton nucleus interactions at $\sqrt{s} = 41.6$ GeV, Phys. Rev. D **79**, 012001 (2009).

[21] A. Adare *et al.* (PHENIX Collaboration), Nuclear Modification of ψ', χ_c, and J/ψ Production in d+Au Collisions, Phys. Rev. Lett. **111**, 202301 (2013).

[22] A. A. Alves Jr. *et al.* (LHCb Collaboration), The LHCb detector at the LHC, J. Instrum. **3**, S08005 (2008).

[23] R. Aaij *et al.* (LHCb Collaboration), LHCb detector performance, Int. J. Mod. Phys. A **30**, 1530022 (2015).

[24] P. A. Zyla *et al.* (Particle Data Group Collaboration), Review of particle physics, Prog. Theor. Exp. Phys. **2020**, 083C01 (2020).

[25] R. Aaij *et al.*, Selection and processing of calibration samples to measure the particle identification performance of the LHCb experiment in Run 2, Eur. Phys. J. Tech. Instrum. **6**, 1 (2019).

[26] A. Betata *et al.*, Calibration and performance of the LHCb calorimeters in Run 1 and 2 at the LHC, arXiv:2008.11556.

[27] T. Sjöstrand, S. Mrenna, and P. Skands, A brief introduction to PYTHIA 8.1, Comput. Phys. Commun. **178**, 852 (2008).

[28] I. Belyaev *et al.*, Handling of the generation of primary events in Gauss, the LHCb simulation framework, J. Phys.: Conf. Ser. **331**, 032047 (2011).

[29] T. Pierog, I. Karpenko, J. M. Katzy, E. Yatsenko, and K. Werner, EPOS LHC: Test of collective hadronization with data measured at the CERN Large Hadron Collider, Phys. Rev. C **92**, 034906 (2015).

[30] D. J. Lange, The EvtGen particle decay simulation package, Nucl. Instrum. Methods Phys. Res., Sect. A **462**, 152 (2001).

[31] N. Davidson, T. Przedzinski, and Z. Was, PHOTOS interface in C++: Technical and physics documentation, Comput. Phys. Commun. **199**, 86 (2016).

[32] J. Allison *et al.* (Geant4 Collaboration), Geant4 developments and applications, IEEE Trans. Nucl. Sci. **53**, 270 (2006); S. Agostinelli *et al.* (Geant4 Collaboration), Geant4: A simulation toolkit, Nucl. Instrum. Methods Phys. Res., Sect. A **506**, 250 (2003).

[33] M. Clemencic *et al.*, The LHCb simulation application, Gauss: Design, evolution and experience, J. Phys.: Conf. Ser. **331**, 032023 (2011).

[34] M. Pivk and F. R. Le Diberder, sPlot: A statistical tool to unfold data distributions, Nucl. Instrum. Methods Phys. Res., Sect. A **555**, 356 (2005).

[35] S. Acharya *et al.* (ALICE Collaboration), Energy dependence of forward-rapidity J/ψ and $\psi(2S)$ production in pp collisions at the LHC, Eur. Phys. J. C **77**, 392 (2017).

R. Aaij,[32] C. Abellán Beteta,[50] T. Ackernley,[60] B. Adeva,[46] M. Adinolfi,[54] H. Afsharnia,[9] C. A. Aidala,[85] S. Aiola,[25]
Z. Ajaltouni,[9] S. Akar,[65] J. Albrecht,[15] F. Alessio,[48] M. Alexander,[59] A. Alfonso Albero,[45] Z. Aliouche,[62] G. Alkhazov,[38]
P. Alvarez Cartelle,[55] S. Amato,[2] Y. Amhis,[11] L. An,[48] L. Anderlini,[22] A. Andreianov,[38] M. Andreotti,[21] F. Archilli,[17]
A. Artamonov,[44] M. Artuso,[68] K. Arzymatov,[42] E. Aslanides,[10] M. Atzeni,[50] B. Audurier,[12] S. Bachmann,[17] M. Bachmayer,[49]
J. J. Back,[56] S. Baker,[61] P. Baladron Rodriguez,[46] V. Balagura,[12] W. Baldini,[21,48] J. Baptista Leite,[1] R. J. Barlow,[62] S. Barsuk,[11]
W. Barter,[61] M. Bartolini,[24] F. Baryshnikov,[82] J. M. Basels,[14] G. Bassi,[29] B. Batsukh,[68] A. Battig,[15] A. Bay,[49] M. Becker,[15]
F. Bedeschi,[29] I. Bediaga,[1] A. Beiter,[68] V. Belavin,[42] S. Belin,[27] V. Bellee,[49] K. Belous,[44] I. Belov,[40] I. Belyaev,[41]
G. Bencivenni,[23] E. Ben-Haim,[13] A. Berezhnoy,[40] R. Bernet,[50] D. Berninghoff,[17] H. C. Bernstein,[68] C. Bertella,[48]
A. Bertolin,[28] C. Betancourt,[50] F. Betti,[20,d] Ia. Bezshyiko,[50] S. Bhasin,[54] J. Bhom,[35] L. Bian,[73] M. S. Bieker,[15] S. Bifani,[53]
P. Billoir,[13] M. Birch,[61] F. C. R. Bishop,[55] A. Bitadze,[62] A. Bizzeti,[22,k] M. Bjørn,[63] M. P. Blago,[48] T. Blake,[56] F. Blanc,[49]
S. Blusk,[68] D. Bobulska,[59] J. A. Boelhauve,[15] O. Boente Garcia,[46] T. Boettcher,[64] A. Boldyrev,[81] A. Bondar,[43] N. Bondar,[38,48]
S. Borghi,[62] M. Borisyak,[42] M. Borsato,[17] J. T. Borsuk,[35] S. A. Bouchiba,[49] T. J. V. Bowcock,[60] A. Boyer,[48] C. Bozzi,[21]
M. J. Bradley,[61] S. Braun,[66] A. Brea Rodriguez,[46] M. Brodski,[48] J. Brodzicka,[35] A. Brossa Gonzalo,[56] D. Brundu,[27]
A. Buonaura,[50] C. Burr,[48] A. Bursche,[27] A. Butkevich,[39] J. S. Butter,[32] J. Buytaert,[48] W. Byczynski,[48] S. Cadeddu,[27] H. Cai,[73]
R. Calabrese,[21,f] L. Calefice,[15,13] L. Calero Diaz,[23] S. Cali,[23] R. Calladine,[53] M. Calvi,[26,j] M. Calvo Gomez,[84]
P. Camargo Magalhaes,[54] A. Camboni,[45,84] P. Campana,[23] A. F. Campoverde Quezada,[6] S. Capelli,[26,j] L. Capriotti,[20,d]
A. Carbone,[20,d] G. Carboni,[31] R. Cardinale,[24,h] A. Cardini,[27] I. Carli,[4] P. Carniti,[26,j] L. Carus,[14] K. Carvalho Akiba,[32]
A. Casais Vidal,[46] G. Casse,[60] M. Cattaneo,[48] G. Cavallero,[48] S. Celani,[49] J. Cerasoli,[10] A. J. Chadwick,[60] M. G. Chapman,[54]
M. Charles,[13] Ph. Charpentier,[48] G. Chatzikonstantinidis,[53] C. A. Chavez Barajas,[60] M. Chefdeville,[8] C. Chen,[3] S. Chen,[27]
A. Chernov,[35] V. Chobanova,[46] S. Cholak,[49] M. Chrzaszcz,[35] A. Chubykin,[38] V. Chulikov,[38] P. Ciambrone,[23] M. F. Cicala,[56]
X. Cid Vidal,[46] G. Ciezarek,[48] P. E. L. Clarke,[58] M. Clemencic,[48] H. V. Cliff,[55] J. Closier,[48] J. L. Cobbledick,[62] V. Coco,[48]
J. A. B. Coelho,[11] J. Cogan,[10] E. Cogneras,[9] L. Cojocariu,[37] P. Collins,[48] T. Colombo,[48] L. Congedo,[19,c] A. Contu,[27]
N. Cooke,[53] G. Coombs,[59] G. Corti,[48] C. M. Costa Sobral,[56] B. Couturier,[48] D. C. Craik,[64] J. Crkovská,[67] M. Cruz Torres,[1]
R. Currie,[58] C. L. Da Silva,[67] E. Dall'Occo,[15] J. Dalseno,[46] C. D'Ambrosio,[48] A. Danilina,[41] P. d'Argent,[48] A. Davis,[62]

O. De Aguiar Francisco,[62] K. De Bruyn,[78] S. De Capua,[62] M. De Cian,[49] J. M. De Miranda,[1] L. De Paula,[2] M. De Serio,[19,c]
D. De Simone,[50] P. De Simone,[23] J. A. de Vries,[79] C. T. Dean,[67] D. Decamp,[8] L. Del Buono,[13] B. Delaney,[55]
H.-P. Dembinski,[15] A. Dendek,[34] V. Denysenko,[50] D. Derkach,[81] O. Deschamps,[9] F. Desse,[11] F. Dettori,[27,e] B. Dey,[73]
P. Di Nezza,[23] S. Didenko,[82] L. Dieste Maronas,[46] H. Dijkstra,[48] V. Dobishuk,[52] A. M. Donohoe,[18] F. Dordei,[27]
A. C. dos Reis,[1] L. Douglas,[59] A. Dovbnya,[51] A. G. Downes,[8] K. Dreimanis,[60] M. W. Dudek,[35] L. Dufour,[48] V. Duk,[77]
P. Durante,[48] J. M. Durham,[67] D. Dutta,[62] M. Dziewiecki,[17] A. Dziurda,[35] A. Dzyuba,[38] S. Easo,[57] U. Egede,[69] V. Egorychev,[41]
S. Eidelman,[43,v] S. Eisenhardt,[58] S. Ek-In,[49] L. Eklund,[59,w] S. Ely,[68] A. Ene,[37] E. Epple,[67] S. Escher,[14] J. Eschle,[50] S. Esen,[32]
T. Evans,[48] A. Falabella,[20] J. Fan,[3] Y. Fan,[6] B. Fang,[73] S. Farry,[60] D. Fazzini,[26,j] P. Fedin,[41] M. Féo,[48] P. Fernandez Declara,[48]
A. Fernandez Prieto,[46] J. M. Fernandez-tenllado Arribas,[45] F. Ferrari,[20,d] L. Ferreira Lopes,[49] F. Ferreira Rodrigues,[2]
S. Ferreres Sole,[32] M. Ferrillo,[50] M. Ferro-Luzzi,[48] S. Filippov,[39] R. A. Fini,[19] M. Fiorini,[21,f] M. Firlej,[34] K. M. Fischer,[63]
C. Fitzpatrick,[62] T. Fiutowski,[34] F. Fleuret,[12] M. Fontana,[13] F. Fontanelli,[24,h] R. Forty,[48] V. Franco Lima,[60] M. Franco Sevilla,[66]
M. Frank,[48] E. Franzoso,[21] G. Frau,[17] C. Frei,[48] D. A. Friday,[59] J. Fu,[25] Q. Fuehring,[15] W. Funk,[48] E. Gabriel,[32] T. Gaintseva,[42]
A. Gallas Torreira,[46] D. Galli,[20,d] S. Gambetta,[58,48] Y. Gan,[3] M. Gandelman,[2] P. Gandini,[25] Y. Gao,[5] M. Garau,[27]
L. M. Garcia Martin,[56] P. Garcia Moreno,[45] J. García Pardiñas,[26,j] B. Garcia Plana,[46] F. A. Garcia Rosales,[12] L. Garrido,[45]
C. Gaspar,[48] R. E. Geertsema,[32] D. Gerick,[17] L. L. Gerken,[15] E. Gersabeck,[62] M. Gersabeck,[62] T. Gershon,[56] D. Gerstel,[10]
Ph. Ghez,[8] V. Gibson,[55] H. K. Giemza,[36] M. Giovannetti,[23,p] A. Gioventù,[46] P. Gironella Gironell,[45] L. Giubega,[37]
C. Giugliano,[21,48,f] K. Gizdov,[58] E. L. Gkougkousis,[48] V. V. Gligorov,[13] C. Göbel,[70] E. Golobardes,[84] D. Golubkov,[41]
A. Golutvin,[61,82] A. Gomes,[1,a] S. Gomez Fernandez,[45] F. Goncalves Abrantes,[63] M. Goncerz,[35] G. Gong,[3] P. Gorbounov,[41]
I. V. Gorelov,[40] C. Gotti,[26] E. Govorkova,[48] J. P. Grabowski,[17] R. Graciani Diaz,[45] T. Grammatico,[13] L. A. Granado Cardoso,[48]
E. Graugés,[45] E. Graverini,[49] G. Graziani,[22] A. Grecu,[37] L. M. Greeven,[32] P. Griffith,[21,f] L. Grillo,[62] S. Gromov,[82]
B. R. Gruberg Cazon,[63] C. Gu,[3] M. Guarise,[21] P. A. Günther,[17] E. Gushchin,[39] A. Guth,[14] Y. Guz,[44,48] T. Gys,[48]
T. Hadavizadeh,[69] G. Haefeli,[49] C. Haen,[48] J. Haimberger,[48] T. Halewood-leagas,[60] P. M. Hamilton,[66] Q. Han,[7] X. Han,[17]
T. H. Hancock,[63] S. Hansmann-Menzemer,[17] N. Harnew,[63] T. Harrison,[60] C. Hasse,[48] M. Hatch,[48] J. He,[6,b] M. Hecker,[61]
K. Heijhoff,[32] K. Heinicke,[15] A. M. Hennequin,[48] K. Hennessy,[60] L. Henry,[25,47] J. Heuel,[14] A. Hicheur,[2] D. Hill,[49] M. Hilton,[62]
S. E. Hollitt,[15] J. Hu,[17] J. Hu,[72] W. Hu,[7] W. Huang,[6] X. Huang,[73] W. Hulsbergen,[32] R. J. Hunter,[56] M. Hushchyn,[81]
D. Hutchcroft,[60] D. Hynds,[32] P. Ibis,[15] M. Idzik,[34] D. Ilin,[38] P. Ilten,[65] A. Inglessi,[38] A. Ishteev,[82] K. Ivshin,[38] R. Jacobsson,[48]
S. Jakobsen,[48] E. Jans,[32] B. K. Jashal,[47] A. Jawahery,[66] V. Jevtic,[15] M. Jezabek,[35] F. Jiang,[3] M. John,[63] D. Johnson,[48]
C. R. Jones,[55] T. P. Jones,[56] B. Jost,[48] N. Jurik,[48] S. Kandybei,[51] Y. Kang,[3] M. Karacson,[48] M. Karpov,[81] N. Kazeev,[81]
F. Keizer,[55,48] M. Kenzie,[56] T. Ketel,[33] B. Khanji,[15] A. Kharisova,[83] S. Kholodenko,[44] K. E. Kim,[68] T. Kirn,[14] V. S. Kirsebom,[49]
O. Kitouni,[64] S. Klaver,[32] K. Klimaszewski,[36] S. Koliiev,[52] A. Kondybayeva,[82] A. Konoplyannikov,[41] P. Kopciewicz,[34]
R. Kopecna,[17] P. Koppenburg,[32] M. Korolev,[40] I. Kostiuk,[32,52] O. Kot,[52] S. Kotriakhova,[38,30] P. Kravchenko,[38] L. Kravchuk,[39]
R. D. Krawczyk,[48] M. Kreps,[56] F. Kress,[61] S. Kretzschmar,[14] P. Krokovny,[43,v] W. Krupa,[34] W. Krzemien,[36] W. Kucewicz,[35,t]
M. Kucharczyk,[35] V. Kudryavtsev,[43,v] H. S. Kuindersma,[32] G. J. Kunde,[67] T. Kvaratskheliya,[41] D. Lacarrere,[48] G. Lafferty,[62]
A. Lai,[27] A. Lampis,[27] D. Lancierini,[50] J. J. Lane,[62] R. Lane,[54] G. Lanfranchi,[23] C. Langenbruch,[14] J. Langer,[15]
O. Lantwin,[50,82] T. Latham,[56] F. Lazzari,[29,q] R. Le Gac,[10] S. H. Lee,[85] R. Lefèvre,[9] A. Leflat,[40] S. Legotin,[82] O. Leroy,[10]
T. Lesiak,[35] B. Leverington,[17] H. Li,[72] L. Li,[63] P. Li,[17] Y. Li,[4] Y. Li,[4] Z. Li,[68] X. Liang,[68] T. Lin,[61] R. Lindner,[48] V. Lisovskyi,[15]
R. Litvinov,[27] G. Liu,[72] H. Liu,[6] S. Liu,[4] X. Liu,[3] A. Loi,[27] J. Lomba Castro,[46] I. Longstaff,[59] J. H. Lopes,[2] G. H. Lovell,[55]
Y. Lu,[4] D. Lucchesi,[28,l] S. Luchuk,[39] M. Lucio Martinez,[32] V. Lukashenko,[32] Y. Luo,[3] A. Lupato,[62] E. Luppi,[21,f] O. Lupton,[56]
A. Lusiani,[29,m] X. Lyu,[6] L. Ma,[4] R. Ma,[6] S. Maccolini,[20,d] F. Machefert,[11] F. Maciuc,[37] V. Macko,[49] P. Mackowiak,[15]
S. Maddrell-Mander,[54] O. Madejczyk,[34] L. R. Madhan Mohan,[54] O. Maev,[38] A. Maevskiy,[81] D. Maisuzenko,[38]
M. W. Majewski,[34] J. J. Malczewski,[35] S. Malde,[63] B. Malecki,[48] A. Malinin,[80] T. Maltsev,[43,v] H. Malygina,[17] G. Manca,[27,e]
G. Mancinelli,[10] R. Manera Escalero,[45] D. Manuzzi,[20,d] D. Marangotto,[25,i] J. Maratas,[9,s] J. F. Marchand,[8] U. Marconi,[20]
S. Mariani,[22,48,g] C. Marin Benito,[11] M. Marinangeli,[49] P. Marino,[49,m] J. Marks,[17] P. J. Marshall,[60] G. Martellotti,[30]
L. Martinazzoli,[48,j] M. Martinelli,[26,j] D. Martinez Santos,[46] F. Martinez Vidal,[47] A. Massafferri,[1] M. Materok,[14] R. Matev,[48]
A. Mathad,[50] Z. Mathe,[48] V. Matiunin,[41] C. Matteuzzi,[26] K. R. Mattioli,[85] A. Mauri,[32] E. Maurice,[12] J. Mauricio,[45]
M. Mazurek,[36] M. McCann,[61] L. Mcconnell,[18] T. H. Mcgrath,[62] A. McNab,[62] R. McNulty,[18] J. V. Mead,[60] B. Meadows,[65]
C. Meaux,[10] G. Meier,[15] N. Meinert,[76] D. Melnychuk,[36] S. Meloni,[26,j] M. Merk,[32,79] A. Merli,[25] L. Meyer Garcia,[2]
M. Mikhasenko,[48] D. A. Milanes,[74] E. Millard,[56] M. Milovanovic,[48] M.-N. Minard,[8] L. Minzoni,[21,f] S. E. Mitchell,[58]
B. Mitreska,[62] D. S. Mitzel,[48] A. Mödden,[15] R. A. Mohammed,[63] R. D. Moise,[61] T. Mombächer,[15] I. A. Monroy,[74] S. Monteil,[9]
M. Morandin,[28] G. Morello,[23] M. J. Morello,[29,m] J. Moron,[34] A. B. Morris,[75] A. G. Morris,[56] R. Mountain,[68] H. Mu,[3]
F. Muheim,[58,48] M. Mukherjee,[7] M. Mulder,[48] D. Müller,[48] K. Müller,[50] C. H. Murphy,[63] D. Murray,[62] P. Muzzetto,[27,48]
P. Naik,[54] T. Nakada,[49] R. Nandakumar,[57] T. Nanut,[49] I. Nasteva,[2] M. Needham,[58] I. Neri,[21,i] N. Neri,[25,i] S. Neubert,[75]
N. Neufeld,[48] R. Newcombe,[61] T. D. Nguyen,[49] C. Nguyen-Mau,[49,x] E. M. Niel,[11] S. Nieswand,[14] N. Nikitin,[40] N. S. Nolte,[48]
C. Nunez,[85] A. Oblakowska-Mucha,[34] V. Obraztsov,[44] D. P. O'Hanlon,[54] R. Oldeman,[27,e] M. E. Olivares,[68]
C. J. G. Onderwater,[78] A. Ossowska,[35] J. M. Otalora Goicochea,[2] T. Ovsiannikova,[41] P. Owen,[50] A. Oyanguren,[47] B. Pagare,[56]
P. R. Pais,[48] T. Pajero,[29,48,m] A. Palano,[19] M. Palutan,[23] Y. Pan,[62] G. Panshin,[83] A. Papanestis,[57] M. Pappagallo,[19,c]
L. L. Pappalardo,[21,f] C. Pappenheimer,[65] W. Parker,[66] C. Parkes,[62] C. J. Parkinson,[46] B. Passalacqua,[21] G. Passaleva,[22]
A. Pastore,[19] M. Patel,[61] C. Patrignani,[20,d] C. J. Pawley,[79] A. Pearce,[48] A. Pellegrino,[32] M. Pepe Altarelli,[48] S. Perazzini,[20]

D. Pereima,[41] P. Perret,[9] K. Petridis,[54] A. Petrolini,[24,h] A. Petrov,[80] S. Petrucci,[58] M. Petruzzo,[25] T. T. H. Pham,[68]
A. Philippov,[42] L. Pica,[29,n] M. Piccini,[77] B. Pietrzyk,[8] G. Pietrzyk,[49] M. Pili,[63] D. Pinci,[30] F. Pisani,[48] A. Piucci,[17] Resmi P.
K,[10] V. Placinta,[37] J. Plews,[53] M. Plo Casasus,[46] F. Polci,[13] M. Poli Lener,[23] M. Poliakova,[68] A. Poluektov,[10] N. Polukhina,[82,u]
I. Polyakov,[68] E. Polycarpo,[2] G. J. Pomery,[54] S. Ponce,[48] D. Popov,[6,48] S. Popov,[42] S. Poslavskii,[44] K. Prasanth,[35]
L. Promberger,[48] C. Prouve,[46] V. Pugatch,[52] H. Pullen,[63] G. Punzi,[29,n] W. Qian,[6] J. Qin,[6] R. Quagliani,[13] B. Quintana,[8]
N. V. Raab,[18] R. I. Rabadan Trejo,[10] B. Rachwal,[34] J. H. Rademacker,[54] M. Rama,[29] M. Ramos Pernas,[56] M. S. Rangel,[2]
F. Ratnikov,[42,81] G. Raven,[33] M. Reboud,[8] F. Redi,[49] F. Reiss,[13] C. Remon Alepuz,[47] Z. Ren,[3] V. Renaudin,[63] R. Ribatti,[29]
S. Ricciardi,[57] K. Rinnert,[60] P. Robbe,[11] A. Robert,[13] G. Robertson,[58] A. B. Rodrigues,[49] E. Rodrigues,[60]
J. A. Rodriguez Lopez,[74] A. Rollings,[63] P. Roloff,[48] V. Romanovskiy,[44] M. Romero Lamas,[46] A. Romero Vidal,[46] J. D. Roth,[85]
M. Rotondo,[23] M. S. Rudolph,[68] T. Ruf,[48] J. Ruiz Vidal,[47] A. Ryzhikov,[81] J. Ryzka,[34] J. J. Saborido Silva,[46] N. Sagidova,[38]
N. Sahoo,[56] B. Saitta,[27,e] D. Sanchez Gonzalo,[45] C. Sanchez Gras,[32] R. Santacesaria,[30] C. Santamarina Rios,[46]
M. Santimaria,[23] E. Santovetti,[31,p] D. Saranin,[82] G. Sarpis,[59] M. Sarpis,[75] A. Sarti,[30] C. Satriano,[30,o] A. Satta,[31] M. Saur,[15]
D. Savrina,[41,40] H. Sazak,[9] L. G. Scantlebury Smead,[63] S. Schael,[14] M. Schellenberg,[15] M. Schiller,[59] H. Schindler,[48]
M. Schmelling,[16] B. Schmidt,[48] O. Schneider,[49] A. Schopper,[48] M. Schubiger,[32] S. Schulte,[49] M. H. Schune,[11]
R. Schwemmer,[48] B. Sciascia,[23] A. Sciubba,[23] S. Sellam,[46] A. Semennikov,[41] M. Senghi Soares,[33] A. Sergi,[24,48] N. Serra,[50]
L. Sestini,[28] A. Seuthe,[15] P. Seyfert,[48] D. M. Shangase,[85] M. Shapkin,[44] I. Shchemerov,[82] L. Shchutska,[49] T. Shears,[60]
L. Shekhtman,[43,v] Z. Shen,[5] V. Shevchenko,[80] E. B. Shields,[26,j] E. Shmanin,[82] J. D. Shupperd,[68] B. G. Siddi,[21]
R. Silva Coutinho,[50] G. Simi,[28] S. Simone,[19,c] N. Skidmore,[62] T. Skwarnicki,[68] M. W. Slater,[53] I. Slazyk,[21,f] J. C. Smallwood,[63]
J. G. Smeaton,[55] A. Smetkina,[41] E. Smith,[14] M. Smith,[61] A. Snoch,[32] M. Soares,[20] L. Soares Lavra,[9] M. D. Sokoloff,[65]
F. J. P. Soler,[59] A. Solovev,[38] I. Solovyev,[38] F. L. Souza De Almeida,[2] B. Souza De Paula,[2] B. Spaan,[15] E. Spadaro Norella,[25,i]
P. Spradlin,[59] F. Stagni,[48] M. Stahl,[65] S. Stahl,[48] P. Stefko,[49] O. Steinkamp,[50,82] S. Stemmle,[17] O. Stenyakin,[44] H. Stevens,[15]
S. Stone,[68] M. E. Stramaglia,[49] M. Straticiuc,[37] D. Strekalina,[82] F. Suljik,[63] J. Sun,[27] L. Sun,[73] Y. Sun,[66] P. Svihra,[62]
P. N. Swallow,[53] K. Swientek,[34] A. Szabelski,[36] T. Szumlak,[34] M. Szymanski,[48] S. Taneja,[62] F. Teubert,[48] E. Thomas,[48]
K. A. Thomson,[60] M. J. Tilley,[61] V. Tisserand,[9] S. T'Jampens,[8] M. Tobin,[4] S. Tolk,[48] L. Tomassetti,[21,f] D. Torres Machado,[1]
D. Y. Tou,[13] M. Traill,[59] M. T. Tran,[49] E. Trifonova,[82] C. Trippl,[49] G. Tuci,[29,n] A. Tully,[49] N. Tuning,[32,48] A. Ukleja,[36]
D. J. Unverzagt,[17] E. Ursov,[82] A. Usachov,[32] A. Ustyuzhanin,[42,81] U. Uwer,[17] A. Vagner,[83] V. Vagnoni,[20] A. Valassi,[48]
G. Valenti,[20] N. Valls Canudas,[45] M. van Beuzekom,[32] M. Van Dijk,[49] E. van Herwijnen,[82] C. B. Van Hulse,[18] M. van Veghel,[78]
R. Vazquez Gomez,[46] P. Vazquez Regueiro,[46] C. Vázquez Sierra,[48] S. Vecchi,[21] J. J. Velthuis,[54] M. Veltri,[22,r]
A. Venkateswaran,[68] M. Veronesi,[32] M. Vesterinen,[56] D. Vieira,[65] M. Vieites Diaz,[49] H. Viemann,[76] X. Vilasis-Cardona,[84]
E. Vilella Figueras,[60] P. Vincent,[13] G. Vitali,[29] A. Vollhardt,[50] D. Vom Bruch,[10] A. Vorobyev,[38] V. Vorobyev,[43,v] N. Voropaev,[38]
R. Waldi,[76] J. Walsh,[29] C. Wang,[17] J. Wang,[5] J. Wang,[4] J. Wang,[3] J. Wang,[73] M. Wang,[3] R. Wang,[54] Y. Wang,[7] Z. Wang,[50]
H. M. Wark,[60] N. K. Watson,[53] S. G. Weber,[13] D. Websdale,[61] C. Weisser,[64] B. D. C. Westhenry,[54] D. J. White,[62]
M. Whitehead,[54] D. Wiedner,[15] G. Wilkinson,[63] M. Wilkinson,[68] I. Williams,[55] M. Williams,[64,69] M. R. J. Williams,[58]
F. F. Wilson,[57] W. Wislicki,[36] M. Witek,[35] L. Witola,[17] G. Wormser,[11] S. A. Wotton,[55] H. Wu,[68] K. Wyllie,[48] Z. Xiang,[6]
D. Xiao,[7] Y. Xie,[7] A. Xu,[5] J. Xu,[6] L. Xu,[3] M. Xu,[7] Q. Xu,[6] Z. Xu,[5] Z. Xu,[6] D. Yang,[3] S. Yang,[6] Y. Yang,[6] Z. Yang,[3] Z. Yang,[66]
Y. Yao,[68] L. E. Yeomans,[60] H. Yin,[7] J. Yu,[71] X. Yuan,[68] O. Yushchenko,[44] E. Zaffaroni,[49] K. A. Zarebski,[53] M. Zavertyaev,[16,u]
M. Zdybal,[35] O. Zenaiev,[48] M. Zeng,[3] D. Zhang,[7] L. Zhang,[3] S. Zhang,[5] Y. Zhang,[5] Y. Zhang,[63] A. Zhelezov,[17] Y. Zheng,[6]
X. Zhou,[6] Y. Zhou,[6] X. Zhu,[3] V. Zhukov,[14,40] J. B. Zonneveld,[58] S. Zucchelli,[20,d] D. Zuliani,[28] and G. Zunica[62]

(LHCb Collaboration)

[1] *Centro Brasileiro de Pesquisas Físicas (CBPF), Rio de Janeiro, Brazil*
[2] *Universidade Federal do Rio de Janeiro (UFRJ), Rio de Janeiro, Brazil*
[3] *Center for High Energy Physics, Tsinghua University, Beijing, China*
[4] *Institute Of High Energy Physics (IHEP), Beijing, China*
[5] *School of Physics State Key Laboratory of Nuclear Physics and Technology, Peking University, Beijing, China*
[6] *University of Chinese Academy of Sciences, Beijing, China*
[7] *Institute of Particle Physics, Central China Normal University, Wuhan, Hubei, China*
[8] *Univ. Grenoble Alpes, Univ. Savoie Mont Blanc, CNRS, IN2P3-LAPP, Annecy, France*
[9] *Université Clermont Auvergne, CNRS/IN2P3, LPC, Clermont-Ferrand, France*
[10] *Aix Marseille Univ, CNRS/IN2P3, CPPM, Marseille, France*
[11] *Université Paris-Saclay, CNRS/IN2P3, IJCLab, Orsay, France*
[12] *Laboratoire Leprince-Ringuet, CNRS/IN2P3, Ecole Polytechnique, Institut Polytechnique de Paris, Palaiseau, France*
[13] *LPNHE, Sorbonne Université, Paris Diderot Sorbonne Paris Cité, CNRS/IN2P3, Paris, France*
[14] *I. Physikalisches Institut, RWTH Aachen University, Aachen, Germany*
[15] *Fakultät Physik, Technische Universität Dortmund, Dortmund, Germany*
[16] *Max-Planck-Institut für Kernphysik (MPIK), Heidelberg, Germany*
[17] *Physikalisches Institut, Ruprecht-Karls-Universität Heidelberg, Heidelberg, Germany*

[18]*School of Physics, University College Dublin, Dublin, Ireland*
[19]*INFN Sezione di Bari, Bari, Italy*
[20]*INFN Sezione di Bologna, Bologna, Italy*
[21]*INFN Sezione di Ferrara, Ferrara, Italy*
[22]*INFN Sezione di Firenze, Firenze, Italy*
[23]*INFN Laboratori Nazionali di Frascati, Frascati, Italy*
[24]*INFN Sezione di Genova, Genova, Italy*
[25]*INFN Sezione di Milano, Milano, Italy*
[26]*INFN Sezione di Milano-Bicocca, Milano, Italy*
[27]*INFN Sezione di Cagliari, Monserrato, Italy*
[28]*Universita degli Studi di Padova, Universita e INFN, Padova, Italy*
[29]*INFN Sezione di Pisa, Pisa, Italy*
[30]*INFN Sezione di Roma La Sapienza, Roma, Italy*
[31]*INFN Sezione di Roma Tor Vergata, Roma, Italy*
[32]*Nikhef National Institute for Subatomic Physics, Amsterdam, Netherlands*
[33]*Nikhef National Institute for Subatomic Physics and VU University Amsterdam, Amsterdam, Netherlands*
[34]*AGH - University of Science and Technology, Faculty of Physics and Applied Computer Science, Kraków, Poland*
[35]*Henryk Niewodniczanski Institute of Nuclear Physics Polish Academy of Sciences, Kraków, Poland*
[36]*National Center for Nuclear Research (NCBJ), Warsaw, Poland*
[37]*Horia Hulubei National Institute of Physics and Nuclear Engineering, Bucharest-Magurele, Romania*
[38]*Petersburg Nuclear Physics Institute NRC Kurchatov Institute (PNPI NRC KI), Gatchina, Russia*
[39]*Institute for Nuclear Research of the Russian Academy of Sciences (INR RAS), Moscow, Russia*
[40]*Institute of Nuclear Physics, Moscow State University (SINP MSU), Moscow, Russia*
[41]*Institute of Theoretical and Experimental Physics NRC Kurchatov Institute (ITEP NRC KI), Moscow, Russia*
[42]*Yandex School of Data Analysis, Moscow, Russia*
[43]*Budker Institute of Nuclear Physics (SB RAS), Novosibirsk, Russia*
[44]*Institute for High Energy Physics NRC Kurchatov Institute (IHEP NRC KI), Protvino, Russia, Protvino, Russia*
[45]*ICCUB, Universitat de Barcelona, Barcelona, Spain*
[46]*Instituto Galego de Física de Altas Enerxías (IGFAE), Universidade de Santiago de Compostela, Santiago de Compostela, Spain*
[47]*Instituto de Fisica Corpuscular, Centro Mixto Universidad de Valencia - CSIC, Valencia, Spain*
[48]*European Organization for Nuclear Research (CERN), Geneva, Switzerland*
[49]*Institute of Physics, Ecole Polytechnique Fédérale de Lausanne (EPFL), Lausanne, Switzerland*
[50]*Physik-Institut, Universität Zürich, Zürich, Switzerland*
[51]*NSC Kharkiv Institute of Physics and Technology (NSC KIPT), Kharkiv, Ukraine*
[52]*Institute for Nuclear Research of the National Academy of Sciences (KINR), Kyiv, Ukraine*
[53]*University of Birmingham, Birmingham, United Kingdom*
[54]*H.H. Wills Physics Laboratory, University of Bristol, Bristol, United Kingdom*
[55]*Cavendish Laboratory, University of Cambridge, Cambridge, United Kingdom*
[56]*Department of Physics, University of Warwick, Coventry, United Kingdom*
[57]*STFC Rutherford Appleton Laboratory, Didcot, United Kingdom*
[58]*School of Physics and Astronomy, University of Edinburgh, Edinburgh, United Kingdom*
[59]*School of Physics and Astronomy, University of Glasgow, Glasgow, United Kingdom*
[60]*Oliver Lodge Laboratory, University of Liverpool, Liverpool, United Kingdom*
[61]*Imperial College London, London, United Kingdom*
[62]*Department of Physics and Astronomy, University of Manchester, Manchester, United Kingdom*
[63]*Department of Physics, University of Oxford, Oxford, United Kingdom*
[64]*Massachusetts Institute of Technology, Cambridge, Massachusetts, USA*
[65]*University of Cincinnati, Cincinnati, Ohio, USA*
[66]*University of Maryland, College Park, Maryland, USA*
[67]*Los Alamos National Laboratory (LANL), Los Alamos, New Mexico, USA*
[68]*Syracuse University, Syracuse, New York, USA*
[69]*School of Physics and Astronomy, Monash University, Melbourne, Australia, associated to*[56]
[70]*Pontifícia Universidade Católica do Rio de Janeiro (PUC-Rio), Rio de Janeiro, Brazil, associated to*[2]
[71]*Physics and Micro Electronic College, Hunan University, Changsha City, China, associated to*[7]
[72]*Guangdong Provencial Key Laboratory of Nuclear Science, Institute of Quantum Matter,*
South China Normal University, Guangzhou, China, associated to[3]
[73]*School of Physics and Technology, Wuhan University, Wuhan, China, associated to*[3]
[74]*Departamento de Fisica, Universidad Nacional de Colombia, Bogota, Colombia, associated to*[3]
[75]*Universität Bonn - Helmholtz-Institut für Strahlen und Kernphysik, Bonn, Germany, associated to*[17]

[76]*Institut für Physik, Universität Rostock, Rostock, Germany, associated to*[17]
[77]*INFN Sezione di Perugia, Perugia, Italy, associated to*[21]
[78]*Van Swinderen Institute, University of Groningen, Groningen, Netherlands, associated to*[32]
[79]*Universiteit Maastricht, Maastricht, Netherlands, associated to*[32]
[80]*National Research Centre Kurchatov Institute, Moscow, Russia, associated to*[41]
[81]*National Research University Higher School of Economics, Moscow, Russia, associated to*[42]
[82]*National University of Science and Technology "MISIS", Moscow, Russia, associated to*[41]
[83]*National Research Tomsk Polytechnic University, Tomsk, Russia, associated to*[41]
[84]*DS4DS, La Salle, Universitat Ramon Llull, Barcelona, Spain, associated to*[45]
[85]*University of Michigan, Ann Arbor, Michigan, USA, associated to*[68]

[a]Universidade Federal do Triângulo Mineiro (UFTM), Uberaba-MG, Brazil.
[b]Hangzhou Institute for Advanced Study, UCAS, Hangzhou, China.
[c]Università di Bari, Bari, Italy.
[d]Università di Bologna, Bologna, Italy.
[e]Università di Cagliari, Cagliari, Italy.
[f]Università di Ferrara, Ferrara, Italy.
[g]Università di Firenze, Firenze, Italy.
[h]Università di Genova, Genova, Italy.
[i]Università degli Studi di Milano, Milano, Italy.
[j]Università di Milano Bicocca, Milano, Italy.
[k]Università di Modena e Reggio Emilia, Modena, Italy.
[l]Università di Padova, Padova, Italy.
[m]Scuola Normale Superiore, Pisa, Italy.
[n]Università di Pisa, Pisa, Italy.
[o]Università della Basilicata, Potenza, Italy.
[p]Università di Roma Tor Vergata, Roma, Italy.
[q]Università di Siena, Siena, Italy.
[r]Università di Urbino, Urbino, Italy.
[s]MSU - Iligan Institute of Technology (MSU-IIT), Iligan, Philippines.
[t]AGH - University of Science and Technology, Faculty of Computer Science, Electronics and Telecommunications, Kraków, Poland.
[u]P.N. Lebedev Physical Institute, Russian Academy of Science (LPI RAS), Moscow, Russia.
[v]Novosibirsk State University, Novosibirsk, Russia.
[w]Department of Physics and Astronomy, Uppsala University, Uppsala, Sweden.
[x]Hanoi University of Science, Hanoi, Vietnam.